Synthesis of Bismaleimides Bearing Electron-Donating Chromophores and Their Fluorescence Behavior during Copolymerization

Xin Zhang, Ying-Hua Jin, Hui-Xiang Diao, Fu-Sheng Du, Zi-Chen Li, and Fu-Mian Li*

Department of Polymer Science & Engineering, College of Chemistry & Molecular Engineering, Peking University, Beijing 100871, China

Received April 1, 2002; Revised Manuscript Received January 22, 2003

ABSTRACT: Bismaleimides and bisitaconimides bearing diphenylmethylamine, triphenylamine, or 2,5-diphenyl-1,3,4-oxadiazole chromophore (symbolized as $A_{(=)-D_{(*)}}-A_{(=)}$), as well as their saturated model compounds were synthesized, and their steady-state and time-resolved fluorescence spectra were investigated. These $A_{(=)}-D_{(*)}-A_{(=)}$ monomers display strong intramolecular fluorescence quenching. Their fluorescence quantum yields and lifetimes are generally lower than those of their model compounds. It was found that the electron-poor C═C bond of maleimide and itaconimide units ($A_{(=)}$) plays a key role in the intramolecular quenching, which is correlated to the electron-accepting ability of $A_{(=)}$ and the geometry arrangement between $A_{(=)}$ and electron-donating chromophore ($D_{(*)}$). The intramolecular quenching was attributed to an intramolecular charge transfer interaction, which was confirmed by intermolecular fluorescence quenching and time-resolved fluorescence studies. On the basis of the intramolecular quenching, a new fluorescence approach can be developed to monitor the process of the polymerization and curing of bismaleimides, which can directly reflect the C═C bond consumption during polymerization and curing. The new fluorescence approach can be utilized not only by an intrinsic fluorescence technique but also by an extrinsic fluorescence technique.

Introduction

In recent years, a wide range of vinyl monomers and their polymers bearing various photo- or electroactive chromophores have been studied and applied in the fields of advanced composites, optical materials and devices.[1] Generally, the C═C bond of vinyl monomers was used as a useful tool to attach various photo- or electroactive groups to a polymer backbone. However, little attention was paid to the effect of the polymerizable C═C bond on the photochemical or photophysical behavior of these vinyl monomers and their polymers. We have had long-standing interest in the synthesis and photochemical behavior, including fluorescence and photosensitization behavior, of electron-poor vinyl monomers bearing electron-donating chromophores ($A_{(=)}-D_{(*)}$), and electron-rich vinyl monomers bearing electron-accepting chromophores ($D_{(=)}-A_{(*)}$) as well as their polymers.[2,3,6,24a] The electron-poor vinyl monomers with electron-donating chromophores can be symbolized as $A_{(=)}-D_{(*)}$, where $A_{(=)}$ denotes an electron-accepting C═C bond such as an acrylic C═C bond, and $D_{(*)}$ denotes an electron-donating chromophore. The electron-rich vinyl monomers with electron-accepting chromophores can be symbolized as $D_{(=)}-A_{(*)}$, where $D_{(=)}$ denotes an electron-donating C═C bond such as a vinyloxy C═C bond, and $A_{(*)}$ denotes an electron-accepting chromophore. It has been found that the fluorescence intensities of these monomers are always dramatically lower than those of their corresponding polymers at the same chromophore concentration.[2,3] Recently, Cumpston et al.,[4] Warman and Verhey et al.[5] also separately described a similar phenomenon. In further work, we found that these $A_{(=)}-D_{(*)}$ and $D_{(=)}-A_{(*)}$ monomers can not only initiate their own polymerization without the addition of photoinitiators, but also serve as photoinitiators and photosensitizers to initiate other polymerization.[2d,3] Furthermore, it was found that the photoinitiating efficiency of these $A_{(=)}-D_{(*)}$ and $D_{(=)}-A_{(=)}$ monomers was strongly correlated to the extent of intramolecular fluorescence quenching.[3b]

Among $A_{(=)}-D_{(*)}$ monomers, we also synthesized *N*-(4-*N*′, *N*′-dimethylaminophenyl) maleimide and its copolymer, and investigated their fluorescence behavior.[6] The C═C bond of the maleimide group ($A_{(=)}$) displays strong electron deficiency as compared to an acrylic C═C bond due to the electron-withdrawing effect of two carbonyl groups.

As mentioned above, the exploration of intramolecular quenching had been focused on the $A_{(=)}-D_{(*)}$ and $D_{(=)}-A_{(*)}$ monomers in our previous work. A deeper understanding of the fluorescence behavior of two or more electron-accepting C═C bonds ($A_{(=)}$) attached to one electron-donating chromophore ($D_{(*)}$) was of subsequent interest to us.

Recently, bismaleimide resins have attracted much attention in the fields of advanced composites because of their excellent processing characteristics without the formation of volatile byproducts, and outstanding thermomechanical and flammability behaviors in the finally cured state.[7] Although a variety of bismaleimide derivatives containing rigid or condensed aromatic rings was synthesized for the preparation of bismaleimide resins, studies on their photochemical behavior, especially fluorescence behavior were scarce.

In this article, we report the synthesis of the new types of $A_{(=)}-D_{(*)}-A_{(=)}$ monomers, that is, bismaleimides containing electron-donating chromophores (Table 1) and their fluorescence behavior. For comparison, bisitaconimides containing triphenylamine or 2,5-diphenyl-1,3,4-oxadiazole chromophore were also synthesized and studied.

* Corresponding author. Fax: +86-10-6275-2054. Telephone: +86-10-6275-7155. E-mail: fmli@chem.pku.edu.cn.

10.1021/ma0205111 CCC: $25.00
Published on Web 03/11/2003

Table 1. $A_{(=)}-D_{(*)}-A_{(=)}$ Bismaleimides, Bistaconimides, and Their Corresponding Saturated Compounds

Type	Nomenclature	Abbreviation	Structure
$A_{(=)}$-$D_{(*)}$-$A_{(=)}$ Bismaleimides	*N, N*-bis (4-maleimidophenyl) methylamine	**BMMA**	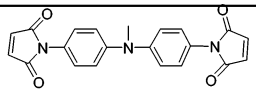
	N, N-bis (4-maleimidophenyl) aniline	**BMPA**	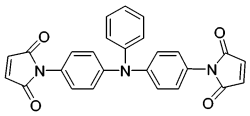
	2, 5-bis (4'-maleimidophenyl) –1, 3, 4-oxadiazole	***p*-BMPO**	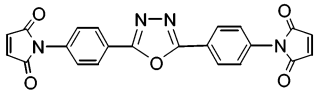
	2, 5-bis (3'-maleimidophenyl) –1, 3, 4-oxadiazole	***m*-BMPO**	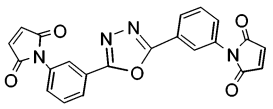
Bissuccinimides	*N, N*-bis (4-succinimidophenyl) methylamine	**BSMA**	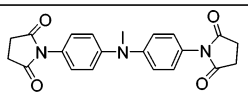
	N, N-bis (4-succinimidophenyl) aniline	**BSPA**	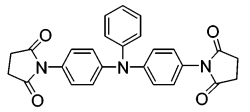
	2, 5-bis (4'-succinimidophenyl) –1, 3, 4-oxadiazole	***p*-BSPO**	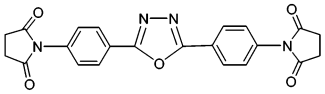
	2, 5-bis (3'-succinimidophenyl) –1, 3, 4-oxadiazole	***m*-BSPO**	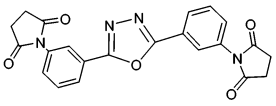
	N, N-bis (4-itaconimidophenyl) aniline	**BIPA**	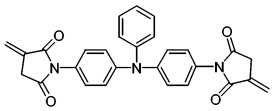
$A_{(=)}$-$D_{(*)}$-$A_{(=)}$ Bisitaconimides	2, 5-bis (4'-itaconimidophenyl –1, 3, 4-oxadiazole	***p*-BIPO**	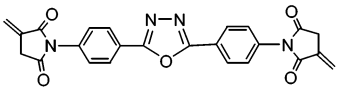
	2, 5-bis (3'-itaconimidophenyl) –1, 3, 4-oxadiazole	***m*-BIPO**	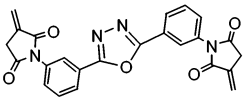

On the other hand, recently, there has been an increasing interest in the development of the on-line monitoring of polymerization, cross-linking or curing by means of fluorescence spectroscopic techniques.[8] Most of the work was performed through the use of a small amount of fluorophore added as a probe to monitor polymerization process, which was the so-called fluorescence probe technique.[8,9] Although the current fluorescence probe technique can provide some useful and referential information on the process of polymerization, it does not give direct information on the conversion of C=C bond during polymerization. In this study, on the basis of the fluorescence behavior of $A_{(=)}-D_{(*)}-A_{(=)}$ monomers, we attempt to develop a new approach toward the fluorescence monitoring of polymerization or cure reaction.

Experimental Section

Materials and Measurements. *p*-Nitrofluorobenzene was purchased from Aldrich. All other chemicals were purchased from Beijing Chemicals Co, and used without further purification. UV−vis absorption spectra were recorded on a Shimadzu UV-250 spectrophotometer. The steady-state fluorescence spectra were recorded on a Hitachi F-4500 fluorescence spectrophotometer at room temperature. The slit width of both monochromators was 5.0 nm. The time-resolved fluorescence measurements were preformed using the time-correlated single-photon counting technique following excitation by a nanosencond flash lamp (Edinburgh Instruments FL900). Fluorescence decay curves were analyzed using a least-squares interactive convolution. All the solvents used were purified to eliminate the interfering impurities for fluorescence measurement. ^{1}H NMR spectra were collected on a Varian Mercury 200 MHz and Bruker 400 MHz spectrometers using chloroform-

d, acetone-d_6, or dimethyl-d_6 sulfoxide as solvents and tetramethylsilane as an internal standard. Infrared spectra were recorded on a Nicolet Magna 750 Fourier transform infrared (FT-IR) spectrometer. Elementary analyses were performed on a Carlo Erba elementary analyzer. Melting points were determined using either a Thomas-Hoover melting point apparatus or a Perkin-Elmer DSC-4 differential scanning calorimeter (heating rate of 10 °C/min). Number- and weight-average molecular weights were estimated using two (30 cm × 75 cm) Burdick and Jackson GPC columns (10^5 Å, 10 μm and 500 Å, 5 μm, respectively) at 35 °C. Degassed DMF was used as eluent at a flow rate of 1.0 mL/min.

Synthesis of Monomers and Model Compounds. *N,N*-Bis(4-maleimidophenyl)methylamine (BMMA). BMMA was prepared by a two-step procedure as follows: (1) A solution of 4,4′-diaminodiphenylmethylamine (1.0 g, 2.7 mmol) in acetone (30 mL) was added dropwise to the acetone (10 mL) solution of maleic anhydride (0.92 g) with stirring at 50 °C for 2 h. A red precipitate appeared in the reaction solution, which was collected by suction filtration. The resulting bismaleamic acid was obtained in yield of 75%. The synthesis of 4,4′-diaminodiphenylmethylamine was described in Supporting Information. (2) A mixture of the above bismaleamic acid (1.5 g), sodium acetate (0.35 g), and acetic anhydride (7.0 mL) was heated at 80 °C for 10 h. Then, the reaction mixture was poured into ice water. A dark brown precipitate was obtained by suction filtration and then was washed twice with 10% sodium carbonate and dried in a vacuum. BMMA was recrystallized twice from ethyl acetate to afford red crystal. Yield: 36.6%. Mp: 220−222 °C. ^{1}H NMR ($CDCl_3$, TMS, ppm): δ 3.346 (s, $-NCH_3$), 7.143−7.245 (dd, 8H, aromatic ring), 6.844 (s, 4H, 2-COCH=CHCO−). IR (KBr pellet, cm^{-1}): 3088.2, 1710.1, 1511.9, 1407.5, 1156.0, 832.8, 688.7. MS (EI): *m/e* 373 (M^+), 319, 261, 54. Anal. Calcd for $C_{21}N_3H_{15}O_4$: C, 67.56; N, 11.25; H, 4.05. Found: C, 67.40; N, 10.88; H, 4.21.

***N,N*-Bis(4-maleimidophenyl)aniline(BMPA).** BMPA was prepared in a similar manner as BMMA except for the aromatic diamine 4,4′-diaminotriphenylamine, which was synthesized as described in Supporting Information. BMPA was recrystallized twice from ethyl acetate to yield yellow crystals. Mp: 256−258 °C. ^{1}H NMR ($CDCl_3$, TMS, ppm): δ 6.88 (s, 4H, 2-CO−CH=CH−CO−), 7.091−7.34 (m, 13H, aromatic ring). MS (EI): *m/e* 435(M^+), 218, 77, 43. IR (KBr pellet, cm^{-1}) 3464.2; 3102.0; 1709.8; 1589.3; 1509.4; 1321.7; 1400.0; 1272.1; 1151.0; 836.5; 688.9. Anal. Calcd for $C_{26}H_{17}N_3O_4$: C, 71.72; N, 9.65; H, 3.94. Found: C, 71.09; N, 9.08; H, 3.96.

The syntheses of other compounds were referred to BMMA. The synthetic procedures and spectral confirmations for *N,N*-bis(4-succinimidophenyl)methylamine (BSMA), *N,N*-bis(4-succinimidophenyl)aniline (BSPA), *N,N*-bis(4-itaconimidophenyl) aniline (BIPA), 2,5-bis(4′-maleimidophenyl)-1,3,4-oxadiazole (*p*-BMPO), 2,5-bis(4′-succinimidophenyl)-1,3,4-oxadiazole (*p*-BSPO), 2,5-bis(4′-itaconimidophenyl)-1,3,4-oxadiazole (*p*-BIPO), 2,5-bis(3′-maleimidophenyl)-1,3,4-oxadiazole (*m*-BMPO), 2,5-bis(3′-succinimido-phenyl)-1,3,4-oxadiazole (*m*-BSPO), and 2,5-bis(3′-itaconimidophenyl)-1,3,4-oxadiazole (*m*-BIPO) were provided in the Supporting Information.

Michael Addition Reaction of BMMA with Isobutylamine. The on-line monitoring of the reaction of BMMA with isobutylamine was preformed by means of ^{1}H NMR spectroscopy in a NMR tube at 28 °C. BMMA (0.0019 g, 0.005 mmol) was charged in a NMR tube. A solution of isobutylamine (1 μL) in actone-d_6 (0.5 mL) was added to the NMR tube via a gastight syringe and mixed thoroughly. The tube was then capped with a septum. At regular intervals, ^{1}H NMR spectra were recorded, and 10 μL of the reaction solution was extracted using a gastight syringe, then diluted to 10 mL of *N,N*-dimethylformamide (DMF) for fluorescence measurement.

Copolymerization of BMMA with 1,6-Diaminohexane. BMMA (0.0019 g, 0.005 mmol) was copolymerized with 1,6-diaminohexane (0.0006 g, 0.005 mmol) in acetone-d_6 (0.5 mL) at 28 °C, which was monitored by means of ^{1}H NMR and fluorescence spectroscopy in the same manner as described above.

Copolymerization of 4,4′-Bismaleimidodiphenylmethane with 4,4′-Diaminodiphenylmethane. Glacial acetic acid (20 μl) was added to a solution of 4,4′-bismaleimidodiphenylmethane (0.3586 g, 0.001 mol) and 4,4′-diaminodiphenylmethane (0.1990 g, 0.001 mol) in fresh *m*-cresol (4 mL). The flask with the reaction mixture was immersed in an oil bath kept at 110 °C for 12 h. Then, 200 μl of the reaction mixture was extracted at regular intervals using gastight syringe and poured into menthol (10 mL)/saturated NaCl (10 mL) to give a yellow precipitate, which was then dried in a vacuum for ^{1}H NMR and FI−IR measurements. Afterward, 0.0035 g of the resulting yellow solid was dissolved in 10 mL of DMF for fluorescence measurement. Samples 1 and 2 were prepared by the above procedure except for *p*-BMPO (0.0041 g, 0.01 mmol) and pyrene (0.0020 g, 0.01 mmol) added at the beginning of the copolymerization, respectively.

Cure Reaction. Sample Preparation. A stoichiometric mixture of BMMA (0.0187 g, 0.05 mmol) and 1,6-diaminohexane (0.0058 g, 0.05 mmol) was dissolved in dichloromethane (1.0 mL). Films were prepared by squeezing 5 drops of the above mixture solution into two quartz plates (1.0 cm × 2.0 cm with thickness 1.0 mm) divided by a 1.0 mm spacer, and the solvent was subsequently volatized at room temperature. The fluorescence spectra were taken in the front face configuration before curing and after subsequent curing at regular intervals and cooling the sample to room temperature. Samples for FT-IR monitoring were prepared by spreading two drops of the mixture solution of BMMA and 1,6-diaminohexane on KBr pellets. The thicknesses of these samples were such that the absorbance values did not exceed 1.0.

Results and Discussion

Synthesis of $A_{(=)}$—$D_{(*)}$—$A_{(=)}$ Bismaleimides, Bisitaconimides, and Their Model Compounds. Bismaleimides and bisitaconimides containing triphenylamine, diphenylmethylamine, or 2,5-diphenyl-1,3,4-oxadiazole chromophore as well as their corresponding saturated model compounds (Table 1) were synthesized by the reaction of corresponding aromatic diamines with maleic anhydride, itaconic anhydride or succinic anhydride, followed by thermal cyclization in the presence of sodium acetate and acetic anhydride. The precursors 4,4′-dinitrodiphenylmethylamine and 4,4′-dinitrotriphenylamine were prepared by a modified Ullman condensation,[12a−f] which is a nucleophilic halo-displacement reaction. Another precursor 2,5-bis(3′-nitrophenyl)-1,3,4-oxadiazole was obtained by the cyclocondensation reaction of *m*-nitrobenzoic acid and hydrazine hydrate in polyphosphoric acid.

The representative synthetic routes to $A_{(=)}-D_{(*)}-A_{(=)}$ bismaleimides BMMA and BMPA are shown in Scheme 1. To our best knowledge, the syntheses of these $A_{(=)}-D_{(*)}-A_{(=)}$ monomers except for BMPA (only appeared in a patent)[12g] have not yet been reported in detail.

Steady-State Absorption and Fluorescence Spectroscopy. Effect of Electron-Poor C=C Bond. Figures 1A and 2A show the UV−vis absorption spectra of bismaleimides BMMA and *p*- and *m*-BMPO, bisitaconimides *p*- and *m*-BIPO, and their corresponding saturated compounds bissuccinimides BSMA and *p*- and *m*-BSPO in 1,2-dichloroethane. It is seen that the absorption spectra of these $A_{(=)}-D_{(*)}-A_{(=)}$ monomers are quite close to their model compounds, indicating that the electron-poor C=C bond does not obviously affect their ground states.

In contrast, the fluorescence spectra of these $A_{(=)}-D_{(*)}-A_{(=)}$ monomers show a distinct difference from their corresponding model compounds as shown in Figures 1B and 2B. Almost no or very weak fluorescence was observed for these $A_{(=)}-D_{(*)}-A_{(=)}$ bismaleimides and

Scheme 1. Synthetic Routes to $A_{(=)}-D_{(*)}-A_{(=)}$ Bismaleimides BMMA and BMPA[a]

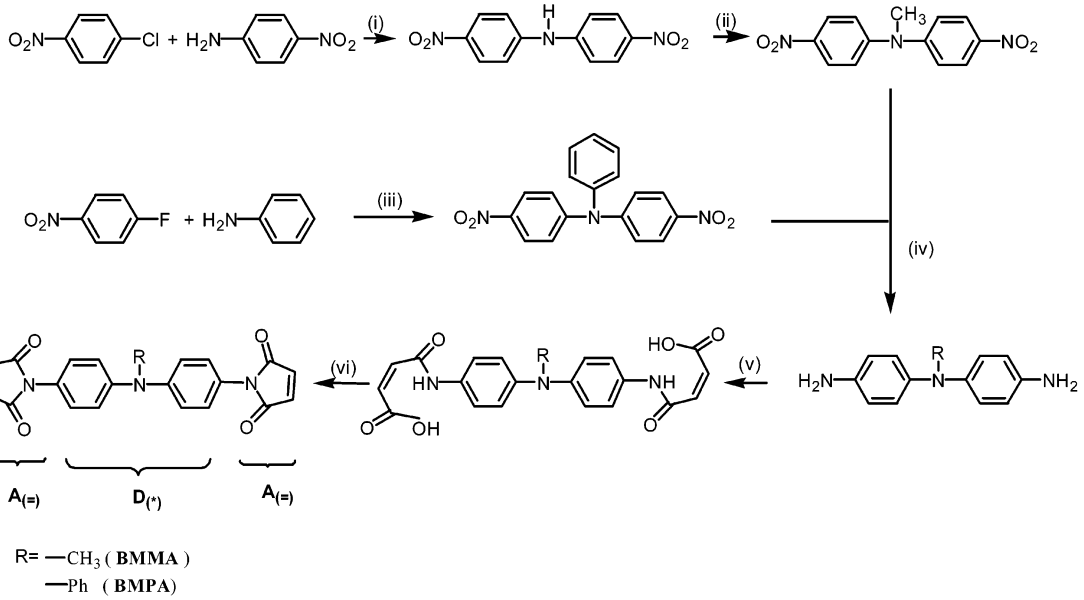

[a] Key: (i) K_2CO_3, DMSO, 1450−150 °C, 5 h; (ii) acetone, CH_3I, reflux; (iii) DMSO, CsF; (iv) Fe, HCl, 50% C_2H_5OH, reflux; (v) acetone, maleic anhydride, 50 °C; (vi) acetic anhydride, AcONa, 80 °C, 10 h.

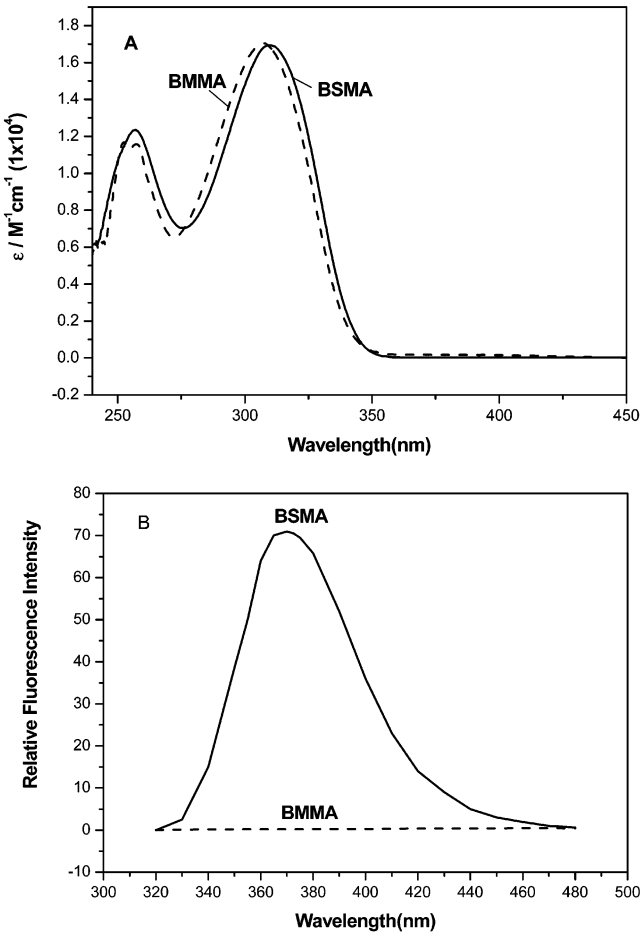

Figure 1. UV−vis absorption spectra (A) and fluorescence spectra (B) of bismaleimide BMMA (- - -) and bissuccinimide BSMA (—) in 1,2-dichloroethane, concentration 5×10^{-5} M.

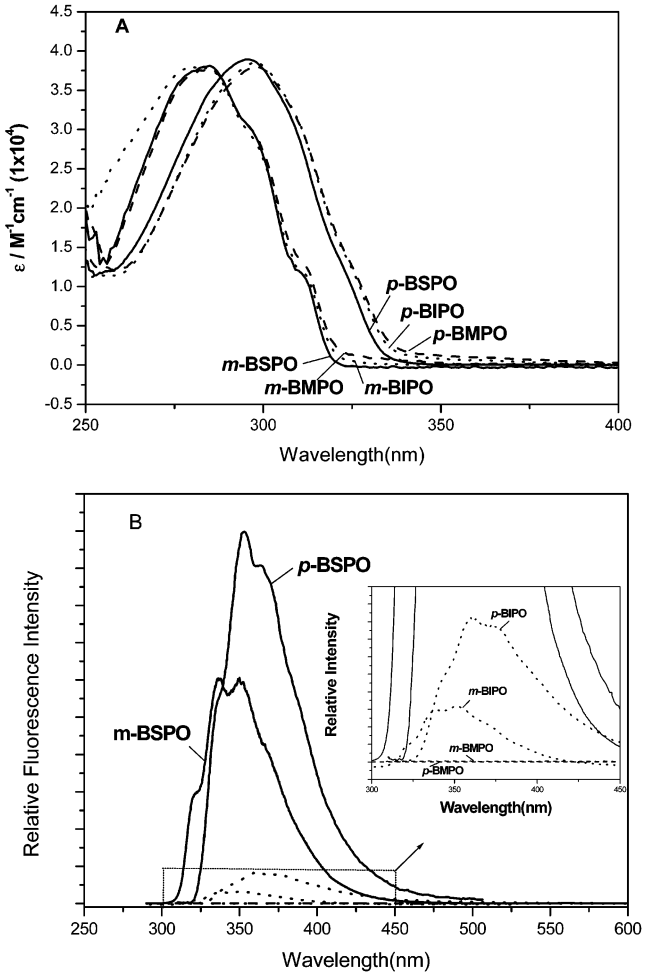

Figure 2. UV−vis absorption (A) and fluorescence spectra (B) of bissuccinimide *p*- and *m*-BSPO (—), bisitaconimide *p*- and *m*-BIPO (•••), and bismaleimide *p*- and *m*-BMPO (- - -) in 1,2-dichloroethane, concentration 3×10^{-5} M.

bisitaconimides, whereas their model compounds display a strong fluorescence at the same chromophore concentration. Such a phenomenon was also observed for BMPA and BSPA as shown in Figure 3. These $A_{(=)}-D_{(*)}-A_{(=)}$ monomers display strong intramolecular fluorescence quenching. The only difference between these $A_{(=)}-D_{(*)}-A_{(=)}$ monomers and their model compounds is the electron-poor C═C bond; therefore, it is believed

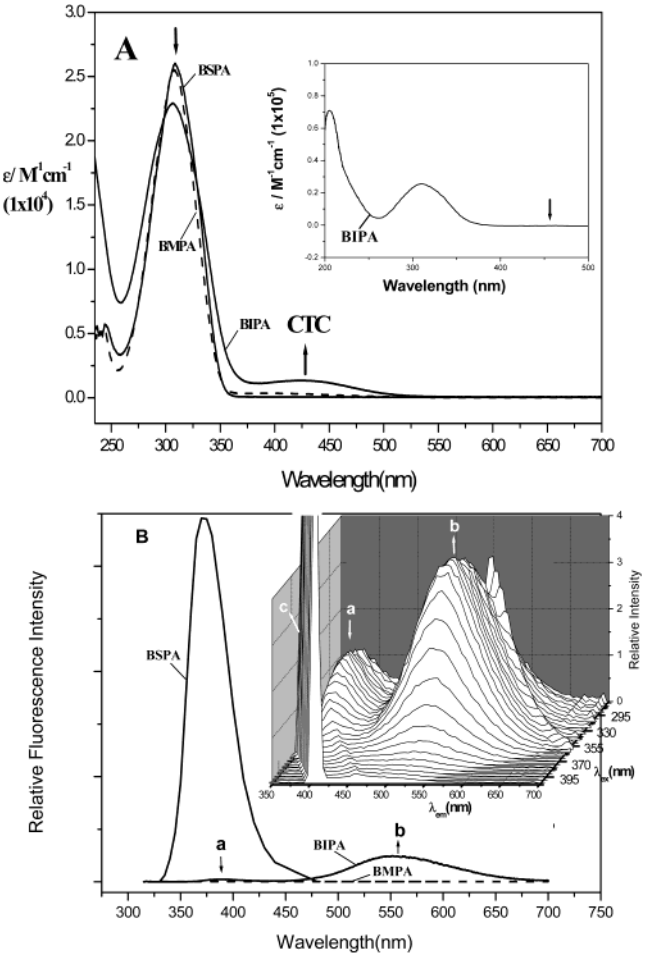

Figure 3. UV−vis absorption (A) and fluorescence spectra (B) of bismaleimide BMMA (- - -) and bissuccinimide BSMA and (—) in 1,2-dichloroethane, concentration 5×10^{-5} M. A. Inset: UV−vis absorption spectra of BIPA in menthol. B. Inset: Three-dimensional fluorescence (emission-excitation-intensity) spectra of BIPA, the emission and excitation of triphenylamine donor (a) and intramolecular charge-transfer complex (b) and the scattered light (c).

that the C═C bond of the maleimide and itaconimide units plays a key role in the intramolecular quenching.

Table 2 lists the spectral data of these compounds in 1,2-dichloroethane. Compared to their model compounds, the fluorescence quantum yields[13] of $A_{(=)}-D_{(*)}-A_{(=)}$ bismaleimides decrease sharply. For $A_{(=)}-D_{(*)}-A_{(=)}$ bisitaconimides, the fluorescence quantum yields decrease by 1−2 orders of magnitude relative to their model compounds. Furthermore, the intramolecular quenching can be quantified by the ratios of fluorescence quantum yields of $A_{(=)}-D_{(*)}-A_{(=)}$ monomers to their corresponding model compounds, which indicates that the intramolecular fluorescence quenching of $A_{(=)}-D_{(*)}-A_{(=)}$ bismaleimides ($\phi_{p-BMPO}/\phi_{p-BSPO} = 1/4990$, $\phi_{m-BMPO}/\phi_{m-BSPO} = 1/6060$) is stronger than that of $A_{(=)}-D_{(*)}-A_{(=)}$ bisitaconimides ($\phi_{p-BIPO}/\phi_{p-BSPO} = 1/12.1$, $\phi_{m-BIPO}/\phi_{m-BSPO} = 1/19.1$). This result can be explained from the electron-drawing strength of maleimide and itaconimide acceptor ($A_{(=)}$). The itaconimide unit can be regarded as an α-substituted acrylamide derivative (EA = 0.565 eV), which shows weaker electron-accepting ability than a maleimide unit (EA = 1.16 eV) according to their electron affinity (EA).[14] Thus, the $A_{(=)}-D_{(*)}-A_{(=)}$ bisitaconimides display relatively weak intramolecular fluorescence quenching. This result suggests that the intramolecular quenching is correlated with the electron-accepting strength of the electron-poor C═C bond ($A_{(=)}$).

Table 2. UV−vis Absorption Maxima ($\lambda_{A,max}$), Extinction Coefficient (ϵ), Fluorescence Emission Maxima ($\lambda_{em,max}$), and Fluorescence Quantum Yields (ϕ_f) and Lifetimes (τ) as Well as the Goodness-of-Fit Parameters (χ_R^2) in 1,2-Dichloroethane

	$\lambda_{A,max}$ (nm)	ϵ ($\times 10^4$) (M^{-1} cm^{-1})	$\lambda_{em,max}$	ϕ_f (%)	τ (ns)	χ_R^2
BMMA	306.9	1.70	*a*	*a*	*a*	
BSMA	310.3	1.69	369.0	7.03	0.85	1.03
BMPA	308.6	2.49	*a*	*a*	*a*	
BSPA	307.5	2.50	372.6	6.92	1.12	1.14
BIPA	308.6	2.25	375.3	0.05	0.91 (12.7%),[b] 0.46 (87.3%)[b]	1.15
	434.5	0.13	530.6	0.50	0.93	1.28
p-BMPO	298.5	3.80	355.7	0.02	*a*	
p-BSPO	296.8	3.85	359.8	8.23	0.26 (84.3%),[b] 1.32 (15.7%)[b]	0.87
m-BMPO	283.2	3.79	336.0	0.01	*a*	
m-BSPO	283.2	3.81	336.0	60.6	0.97	0.86
m-BIPO	281.5	3.80	338.0	3.18	0.24 (75.4%)[b], 1.48 (24.6%)[b]	0.94

[a] No reliable data obtained due to very weak fluorescence. [b] Fractional contribution from each species.

In addition, it is well-known that a 2,5-diphenyl-1,3,4-oxadiazole (DPO) group is generally recognized as an electron-accepting chromophore in the fields of electroluminescence science and technology.[15] However, compared to the model compounds (*p*- and *m*-BSPO), the fluorescence intensities of bismaleimides (*p*- and *m*-BMPO), and bisitaconimides (*p*- and *m*-BIPO) obviously decrease, which also shows intramolecular fluorescence quenching. This implies that an intramolecular interaction occurs between the 2,5-diphenyl-1,3,4-oxadiazole group and the maleimide or itaconimide unit. This result can be analyzed according to the electron-accepting ability of maleimide, itaconimide, and DPO groups. The electron affinity (EA) of maleimide (EA = 1.16 eV)[16] and itaconimide (EA = 0.565 eV)[14] is higher than that of DPO (EA = 0.449 eV).[17] In principle, the higher value of EA represents stronger electron-accepting ability. Therefore, compared to the strong maleimide and itaconimide acceptors ($A_{(=)}$), the DPO group acts as a relative electron donor ($D_{(*)}$). In other words, within the three-unit compounds (*p*- and *m*-BMPO, *p*- and *m*-BIPO), the DPO group displays a relatively electron-donating property, although the EA value of the itaconimide unit is very close to that of the DPO group.

Absorption and Emission of Charge-Transfer Complex (CTC). For BMMA, BMPA and BIPA, interestingly, the absorption at 309.0 nm decreases and becomes broader gradually, a weak absorption band appears in BMPA, and becomes more obvious in BIPA (434.5 nm) as shown in Figure 3A. Accordingly, the fluorescence intensity of BIPA at 375.3 nm decreases, and an obvious broad structureless fluorescence peak was observed at 530.6 nm (Figure 3B). The three-dimensional fluorescence (excitation−emission−intensity) spectra of BIPA are shown in the inset of Figure 3B. The broad absorption and emission bands were caused by an intramolecular charge transfer interaction, which was subsequently confirmed by its disappearance in methanol as shown in the inset of Figure 3A. This is due to the protonation of triphenylamine group to a certain extent in protonic solvents, leading to an invalid electron donor. Hence, the broad structureless absorption and emission are assigned to a CTC formation, which may be involved in an intramolecular multiple

charge-transfer interaction, that is, an intramolecular interaction between multi- maleimide or itaconimide acceptors ($A_{(=)}$) and one triphenylamine donor ($D_{(*)}$). In the case of intermolecular interaction, the absorption and emission of multiple charge transfer are hardly observable, since the dynamic collision occurring among three or four molecules is hardly possible at the same time. This can be further supported by the following intermolecular quenching study. It should be noted that the multiple charge transfer is considerably interesting, which is being explored in our current study on tris-maleimides bearing electron-donating chromophore (symbolized $[A_{(=)}]_3-D_{(*)}$).

For other $A_{(=)}-D_{(*)}-A_{(=)}$ bismaleimides and bisitaconimides, no absorption or emission of charge-transfer complex (CTC) was observed. Thus, although the electron-donating and electron-accepting ability of $D_{(*)}$ and $A_{(=)}$ obviously affect the formation of CTC, a reasonable correlation cannot be obtained between the formation of CTC and the strength of $A_{(=)}$ or $D_{(*)}$. The reason for this may be that the CTC formation was determined not only by the strength of $A_{(=)}$ and $D_{(*)}$ but also by various other factors such as the axial orientation or geometry arrangement between $A_{(=)}$ and $D_{(*)}$.

Influence of the Geometry Arrangement Between $A_{(=)}$ and $D_{(*)}$. For the para series *p*-BMPO, *p*-BIPO, and *p*-BSPO, their absorption and fluorescence spectra generally show red shifts from 14.0 nm to 23.8 nm relative to the meso series *m*-BMPO, *m*-BIPO and *m*-BSPO as shown in Figure 2A and Table 2. The intramolecular quenching of the meso series ($\phi_{m-\mathrm{BMPO}}/\phi_{m-\mathrm{BSPO}} = 1/6060$, $\phi_{m-\mathrm{BIPO}}/\phi_{m-\mathrm{BSPO}} = 1/19.1$) is stronger than that of the para series ($\phi_{p-\mathrm{BMPO}}/\phi_{p-\mathrm{BSPO}}=1/4990$, $\phi_{p-\mathrm{BIPO}}/\phi_{p-\mathrm{BSPO}} = 1/12.1$). Therefore, the geometry arrangement of the para and meso series has to be further analyzed as a factor in the intramolecular quenching. The conformations of energy minimum of the para and meso series were calculated by a semiempirical (AM1) method using a Gaussian98 program, showing that the twisted or dihedral angles between $A_{(=)}$ and $D_{(*)}$ for *m*-BMPO (28.20°) and *m*-BIPO (29.5°) are larger than those of *p*-BMPO (23.9°) and *p*-BIPO (27.7°). A large twisted angle between $A_{(=)}$ and $D_{(*)}$ favors the occurrence of charge separate state,[9d−f] which leads to more obvious intramolecular quenching for meso series.

The above results reveal that the electron-poor C=C bond plays a key role in the intramolecular quenching, which is correlated to the electron-accepting strength of $A_{(=)}$ and the geometry arrangement between $A_{(=)}$ and $D_{(*)}$. The formation of CTC shows that the intramolecular quenching is attributed to an intramolecular charge-transfer interaction.

Time-Resolved Fluorescence Spectroscopy. To further explore the nature of intramolecular quenching, the time-resolved fluorescence decays of these $A_{(=)}-D_{(*)}-A_{(=)}$ monomers and their model compounds were investigated. The fluorescence lifetimes and goodness-of-fit parameters of these compounds are also listed in Table 2. For BSMA, BSPA, and *p*- and *m*-BSPO, their fluorescence decays were well fitted by a single-exponential function. A typical fit is illustrated in Figure 4A. For BMMA, BMPA, and *p*- and *m*-BMPO, no reliable data were obtained due to the very weak fluorescence. For *p*- and *m*-BIPO, a dual exponential fit was observed, which may be due to the existence of two emitting conformations. The average lifetimes of *p*-BIPO

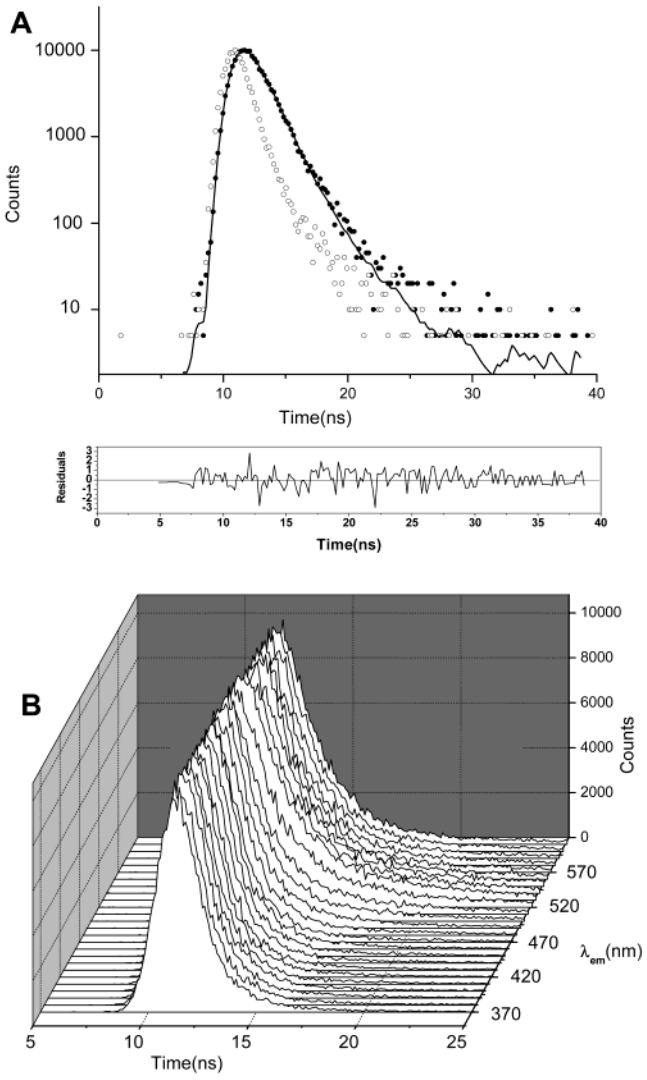

Figure 4. (A) Fluorescence decay curve of BSPA in 1,2-dichloroethane, $\lambda_{ex} = 310.0$ nm, $\lambda_{em} = 375.0$ nm, the flash lamp instrument response profile (○), the experimental fluorescence data points (●), the fitted curve (—), and the residues between the fit and experimental data. Concentration: 5.0×10^{-5} M. (B) Time-resolved fluorescence decay of BIPA, in 1,2-dichloroethane. The excitation wavelength was 310.0 nm and the emission wavelength was varied from 370.0 to 610.0 nm in 10.0 nm steps. Concentration: 5.0×10^{-5} M.

($\langle\tau\rangle = 0.426$ ns) and *m*-BIPO ($\langle\tau\rangle = 0.545$ ns) are shorter than that of their model compounds. Therefore, the intramolecular quenching also results in a shortened fluorescence lifetime. The time-resolved fluorescence spectra of BIPA are shown in Figure 4B. At higher emission wavelengths, the decay curve becomes broader. The fluorescence decay was fitted by dual exponential curve. With increasing emission wavelengths, an increasing amount of relatively longer lifetime was observed. The short lifetime (0.46 ns) is assigned to the reduced emission of triphenylamine donor. The relatively long lifetime (0.93 ns) is assigned to the emission of intramolecular charge-transfer complex. These results confirm that the charge-transfer mechanism of intramolecular quenching.

Intermolecular Fluorescence Quenching. To gain a better understanding of intramolecular quenching, the intermolecular fluorescence quenching of these model compounds by itaconic anhydride and maleic anhydride was investigated. The kinetics of steady-state fluores-

Table 3. Stern−Volmer Constants ($k_q\tau_0$) and Bimolecular Quenching Constants (k_q) of the Fluorescence Quenching of Bissuccimide BSMA, BSPA, and *p*-BSPO by Itaconic Anhydride (IAn) and Maleic Anhydride (MAn)

	quenchers	$k_q\tau_0$ (M^{-1})	k_q (M^{-1} s^{-1})
BSMA	MAn	7.00	8.24×10^9
	IAn	9.53	1.12×10^9
BSPA	MAn	2.78	2.55×10^9
	IAn	2.74	2.51×10^9
p-BSPO	MAn	0.29	2.9×10^8
	IAn	0[a]	0[a]

[a] No fluorescence quenching observed.

cence quenching is described by the Stern−Volmer equation[18a]

$$I_0/I = 1 + K_q\tau_0[Q]$$

where I_0 and τ_0 are the unquenched intensity and lifetime, and [Q] is the quencher concentration. The quenched intensity (I) was corrected to avoid the inner filter effects due to the absorption of quenchers.[18b] It should be noted that the correction for quenched intensity is considerably important, if the absorption of quenchers is near the excitation wavelength. Some unreasonable results can be obtained readily without the correction.[10] The Stern−Volmer plots for the fluorescence quenching were given in the Supporting Information. The Stern−Volmer constant ($K_q\tau_0$) and bimolecular quenching constant (K_q) were calculated and are listed in Table 3.

In principle, k_q reflects the efficiency of fluorescence quenching or the accessibility of the quenchers to the fluorophore. The value k_q for BSMA indicates a diffusion-controlled quenching, which typically leads to the values of k_q near 1×10^{10} M^{-1} s^{-1}.[18a] The smaller values of k_q (10^8−10^9 M^{-1} s^{-1}) for BSPA and *p*-BSPO may be due to the steric shielding and electron-donating strength of the model compounds.

Generally, the smaller values of the ionizing potentials of electron donors represent stronger electron-donating ability. The ionizing potentials of triphenylamine, diphenylmethylamine and 2,5-diphenyl-1,3,4-oxadiazole are 6.86, 6.94, and 9.0 eV, respectively.[19] Thus, the electron-donating ability decreases in the order of BSPA> BSMA > *p*-BSPO. However, the bimolecular quenching constants (k_q) decrease in the order of BSMA > BSPA > *p*-BSPO, which is not consistent with their electron-donating ability. The result can be understood from the steric effect of the chromophore donor. Although the electron-donating ability of triphenylamine group is stronger than that of diphenylmethylamine group, the steric shielding of triphenylamine group is more obvious, which leads to a decrease in the collisional quenching.

Moreover, it was found that the fluorescence intensity of *p*-BSPO was not quenched by itaconic anhydride (Table 3), suggesting that the charge-transfer interaction between *p*-BSPO and itaconic anhydride hardly occurred intermolecularly due to their close electron affinity. However, in the intramolecular case, as described in previous section, the intramolecular quenching occurred obviously in *p*-BIPO and *m*-BIPO ($A_{(=)}$−$D_{(*)}$−$A_{(=)}$). This shows that the intramolecular quenching is a distinct mechanism from the intermolecular quenching as shown in Scheme 2. The intramolecular quenching generally causes a sharp decrease in fluorescence intensities and lifetimes, which is concentration independence. In contrast, the intermolecular quenching may be attributed to a dynamic quenching. There is only a moderate decrease in the fluorescence intensities, which strongly depends on the concentration of fluorophores and quenchers.

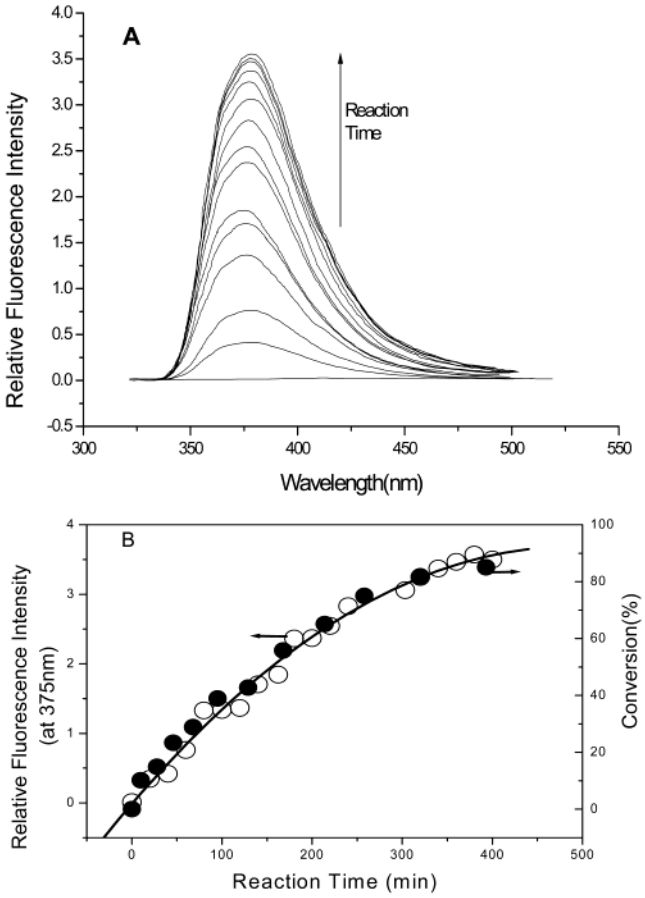

Figure 5. (A) Fluorescence spectra during the reaction of BMMA with isobutylamine at room temperature (λ_{ex} = 310.0 nm). Reaction times for each spectrum (min): 0, 40, 60, 100, 120, 162.5, 180, 200, 220, 240, 303.5, 320, 340, 360, 380, and 400 in the order of increasing fluorescence intensity (from bottom to top). (B) Reaction of BMMA with isobutylamine monitored by following the changes in fluorescence intensity (○) and by means of NMR spectroscopy (●).

Model Reaction. Since the electron-poor C=C bond ($A_{(=)}$) plays a significant role in the intramolecular quenching, the fluorescence intensities of $A_{(=)}$−$D_{(*)}$−$A_{(=)}$ bismaleimides can be expected to increase with the C=C bond consumption. Therefore, the model reaction of BMMA with isobutylamine in acetone was carried out as follows:

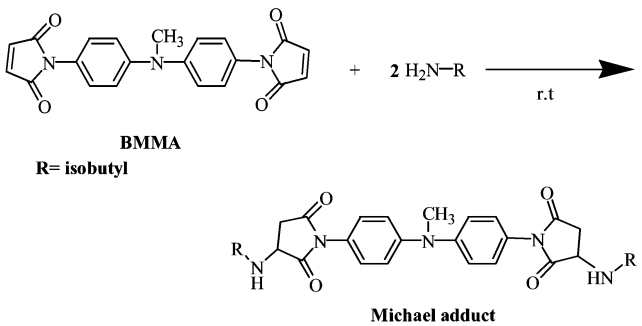

Figure 5A shows that the fluorescence intensity increases gradually during the reaction. This implies

Scheme 2. Proposed Mechanisms for Intermolecular Quenching (a) and Intramolecular Quenching (b)

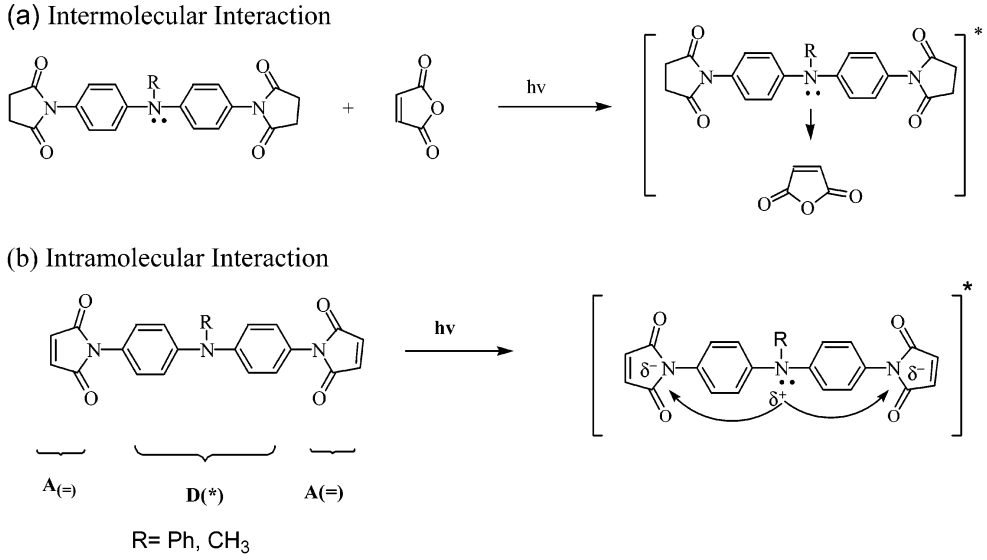

that the C=C bonds of BMMA were consumed gradually leading to the disappearance of intramolecular quenching. To verify the fluorescence data, the changes of C=C bonds during the reaction were monitored by means of ^{1}H NMR spectroscopy. The NMR peak at δ 3.35 (3H of $-CH_3$ adjacent to the N atom of BMMA) was used as a reference. The ^{1}H NMR spectra during the model reaction were provided in Supporting Information. The kinetic curve of the reaction was obtained by calculating periodically the integrals of the peak at δ 7.01 (4H of the C=C bonds of two maleimide ring) during the reaction. The fluorescence data are quite in agreement with the ^{1}H NMR data as shown in Figure 5B. Thus, the consumption of the C=C bonds of these bismaleimides can be estimated by following the change in fluorescence intensity during the reaction.

Copolymerization Monitoring. Recently, fluorescence spectroscopy as a significant tool has been developed for the in situ, on-line monitoring of polymerization, cross-linking, or curing.[8,21−24] The most of information on polymerization was indirectly obtained from the changes in microenvironment such as reduced free volume, polarity, viscosity, etc.[8,9c,24b] Therefore, this often leads to some unsatisfactory reports on polymerization: [20] (1) The fluorescence behavior of probe is no sensitive to the polymerization at the early stage, where almost no changes occur in surrounding media. (2) At the gel effect and/or vitrification stage, the fluorescent signals are grossly magnified due to the dramatically environmental changes.

To overcome the problem mentioned above, Miller et al.,[21] Neckers and Jager et al.,[22] and Pankasem et al.[23] separately used acrylate derivatives bearing fluorine, 4-(dialkylamino)-4′-nitrostilbenes or pyrene fluorophore as fluorescence labels to monitor the polymerization of methyl methacrylate. Likewise, we reported the photopolymerization monitoring of $A_{(=)}-D_{(*)}$ *N*-acryloyl-*N*′-phenylpiperazines by following their fluorescence behavior.[24a] It was found that the fluorescence intensities of the fluorophores of these acrylic labels are only partially or not quenched by their own acrylic C=C bond. Therefore, the fluorescence intensities of unpolymerized acrylic labels also contribute to the overall fluorescence changes during the polymerization. This leads to an obvious error in the polymerization monitoring due to the uncertain amount of these unpolymerized acrylic labels, as these labels become incorporated into polymer chain. Recently, Warman and Verhey et al.[5] reported the use of a maleimide derivative bearing a chromophore as a fluorescence label. However, not only the fluorescence intensity of the maleimide label but also its emission wavelength was changed during polymerization. This caused a complex and difficult monitoring of polymerization.

In this study, we seek a good and convenient approach toward the polymerization monitoring by means of fluorescence spectroscopy. In general, fluorescence spectroscopic techniques can be divided into two classes, an intrinsic fluorescence technique and an extrinsic fluorescence technique. In the following work, the two techniques were employed, respectively.

(a) Intrinsic Fluorescence. Copolymerization of BMMA with 1,6-Diaminohexane. The polyaddition reaction of an equimolar feed of BMMA and 1,6-diaminohexane in acetone at room temperature gave a linear polymer[7] (M_n=6450) with a board polydispersity (PD = 1.7).

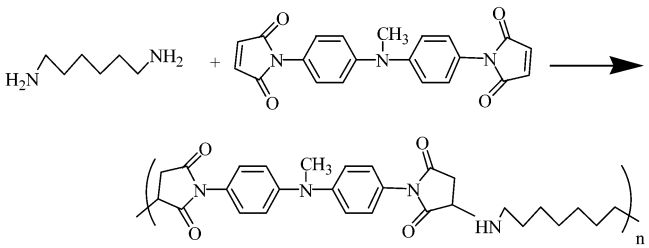

The fluorescence intensity was found to increase rapidly at the beginning of copolymerization, implying that the C=C bond conversion is fast. As the copolymerization proceeds, the increase in fluorescence intensity becomes slower, suggesting the C=C bond conversion becomes lower. At the end of polymerization, the fluorescence intensity does not increase obviously. The dynamic data obtained from the fluorescence intensity were confirmed by ^{1}H NMR spectroscopy.

Figure 6A shows the ^{1}H NMR spectra during the copolymerization of BMMA with 1,6-diaminohexane. It is seen that all ^{1}H NMR peaks become broader during

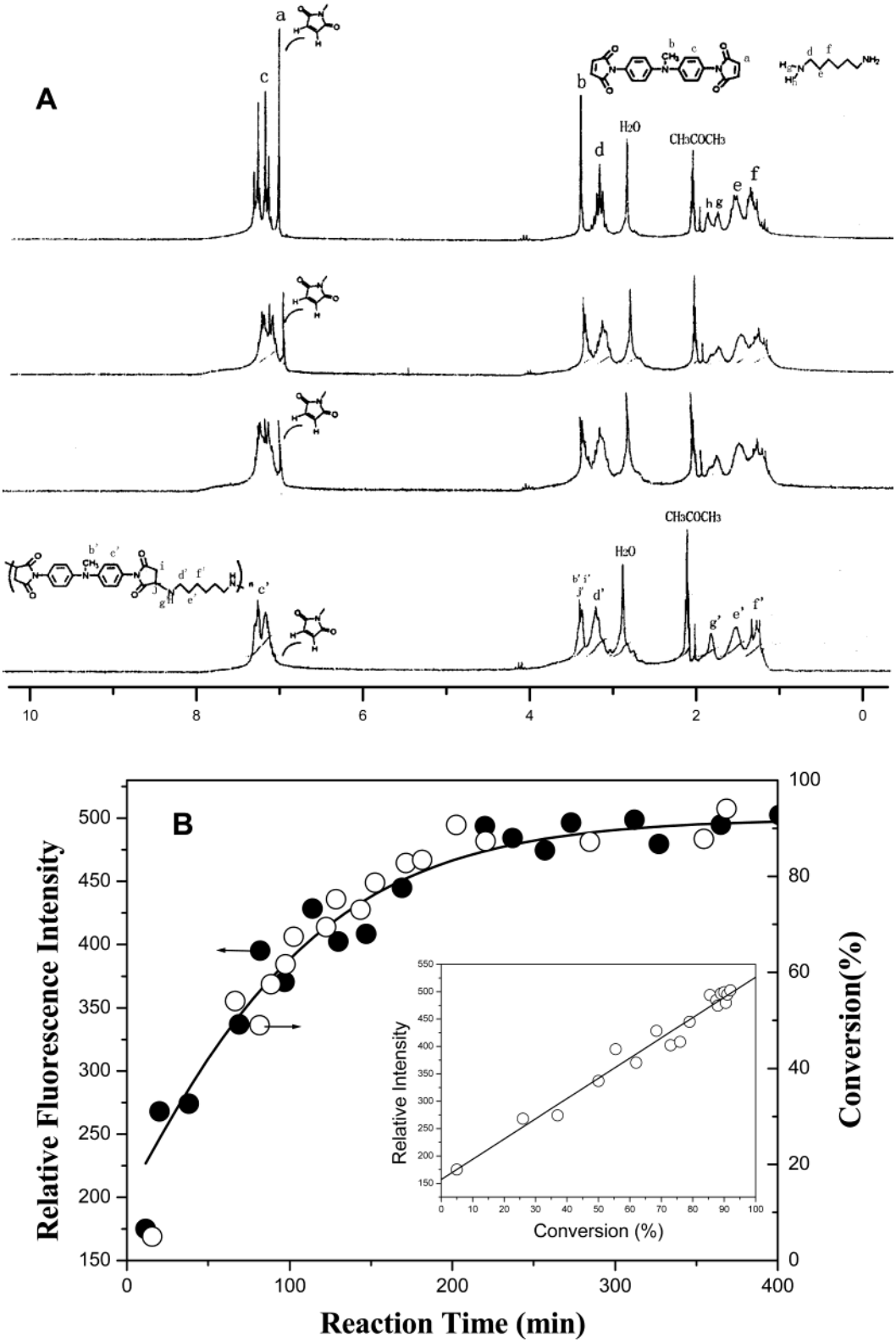

Figure 6. (A) ^{1}H NMR spectra during the copolymerization of BMMA with 1,6-diaminohexane in acetone-d_6, reaction times for each spectrum (min): 0, 66.5, 152.5, 240.0 (from top to bottom). (B) Kinetic curve of the copolymerization obtained from ^{1}H NMR data (○) and fluorescence data (●). Inset: Plot of fluorescence intensity vs the degree of copolymerization.

the polymerization due to the formation of polymer chain. The peak at δ 7.00 (4H of two C═C bonds of BMMA) decreases during the copolymerization, which is used to calculate the consumption of C═C bond by taking the integrals under the peak from δ 7.18 to 7.35 (assigned to 8H of two phenyl rings) as a reference. A good agreement between the fluorescence data and ^{1}H NMR data is shown in Figure 6B. Such a good agreement may be attributed to the strong intramolecular quenching of $A_{(=)}-D_{(*)}-A_{(=)}$ bismaleimides: (1) the very weak fluorescence of BMMA does not contribute to the overall changes in fluorescence intensity during the copolymerization; (2) the fluctuation error in fluorescence intensity is negligible as compared to the pro-

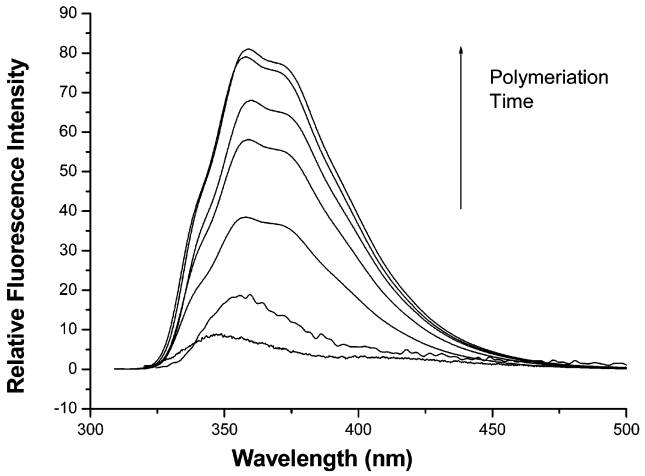

Figure 7. Fluorescence spectra (sample 1) during the copolymerization of 4,4′-bismaleimidodiphenylmethane and 4,4′-diaminodiphenylmethane in *m*-cresol at 110 °C. Reaction times for each spectrum (min): 10, 20, 32, 40, 51, 146, 159 (from bottom to top). [*p*-BMPO] = 6.25×10^{-5} M(λ_{ex}=310.0 nm).

nounced enhancement in fluorescence intensity during the copolymerization. As a result, the increasing fluorescence intensity is exclusively due to the consumption of C═C bonds of BMMA. A linear relationship between the fluorescence intensity and the degree of copolymerization can be obtained as shown in the inset of Figure 6B. Thus, based on the intramolecular quenching, a new fluorescence approach could be developed to directly reflect the C═C bond consumption during the copolymerization of these bismaleimides.

(b) Extrinsic Fluorescence. The above results show that the new fluorescence approach can be employed by an intrinsic fluorescence technique. To pursue a further study, we explore the possibility for an extrinsic fluorescence technique.

4,4′-Bismaleimidodiphenyl methane (BMDPM) and 4,4′-diaminodiphenyl methane (DADPM) were commercially available and widely used as comonomers for bismaleimide resins.[7] The condensation polymerization of an equimolar feed of BMDPM and DADPM gave a linear polymer in *m*-cresol at 110 °C.[25] A small amount (4.1 mg) of *p*-BMPO as an extrinsic label was added to the BMDPM/DADPM system at the beginning of copolymerization (sample 1) as follows:

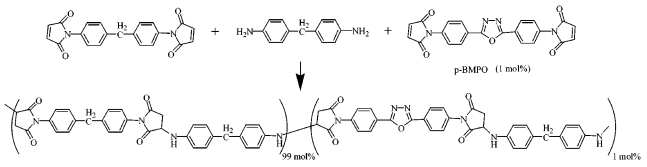

The polymerization process was monitored by ^{1}H NMR spectroscopy according to the change in ^{1}H NMR peak at δ 7.16, using the integrals of the peak at δ 4.03 (assigned to 2H of the methylene unit of DADPM) as an internal reference. The degree of polymerization was also determined by means of FT-IR spectroscopy according to the change in the absorption band at 1183 cm^{-1} using eq 1, which is described in detail in the following cure monitoring.

Figure 7 shows the fluorescence spectra during the copolymerization for sample 1. A fluorescence intensity curve with reaction time was thus obtained, which agreed with the kinetic curve obtained from ^{1}H NMR

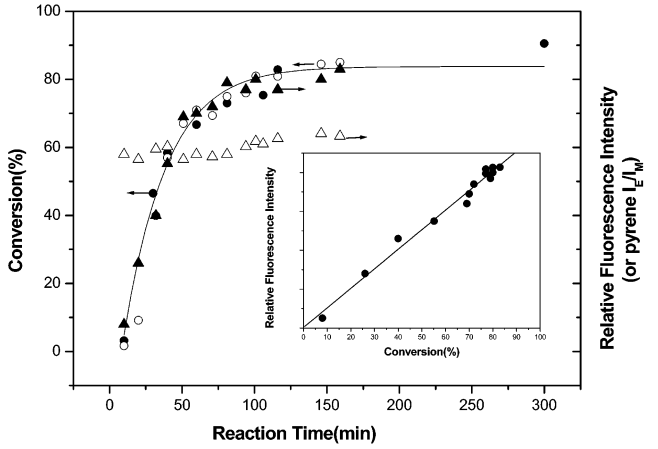

Figure 8. Copolymerization of 4,4′-bismaleimidodiphenylmethane and 4,4′-diaminodiphenylmethane in *m*-cresol monitored by following the changes in fluorescence intensity (sample 1) (▲) (λ_{ex} = 310.0 nm, λ_{em} = 355.0 nm), by extrinsic fluorescence probe technique (sample 2) (△) according to the intensity ratios (IE/IM) of pyrene, λ_{ex} = 345.0 nm, and by means of ^{1}H NMR spectroscopy (●) and FT-IR spectroscopy (○). Inset: Correlation plot between fluorescence and the degree of copolymerization for sample 1.

or IR data as shown in Figure 8. The result suggests that the new fluorescence approach can be also employed by an extrinsic fluorescence technique. In addition, Figure 8 also shows that the IR results are consistent with the ^{1}H NMR results, indicating that the IR method used is reliable in this study.

For comparison, sample 2 was prepared by adding a small amount of pyrene (2.0 mg) into the BMDPM/DADPM system, which is a commonly used fluorescence probe technique.[26,9b] A fluorescence intensity ratio (I_E/I_M) method[9b] was utilized to follow the polymerization process, which was calculated by taking the integrals under the fluorescence spectra from 455.0 to 555.0 nm for the pyrene excimer (I_E), and from 372.0 to 440.0 nm for the pyrene monomer (I_M). There is only a slight change in the intensity ratios of pyrene (I_E/I_M) during the copolymerization (Figure 8), which is no sensitive to the polymerization process. Hence, the currently applied fluorescence probe technique is not suitable for the polymerization monitoring of bismaleimides.

Therefore, compared to the current fluorescence probe technique, the advantage of the new fluorescence approach is that its fluorescence information is derived from C═C bond, not from microenvironment changes.

Cure Monitoring. The monitoring of cure process is important to control and design optimal properties for advanced materials.Various methods such as differential scanning calorimetry (DSC),[24b,27] FT-IR spectroscopy,[28] UV-reflectance spectroscopy,[29,10a] solid-state NMR spectroscopy,[30] and ESR spectroscopy[31] have been utilized to study cross-linking or cure system. Among them, recently, fluorescence spectroscopic techniques have gained an considerable interest as a significant tool for the cross-linking or cure monitoring.[24b,32−34] Neckers and Strehmel et al.[33] used a strong medium-dependent fluorescence probe to monitor photoinduced radical and cationic cross-linking. Sung et al.[10,29b,c,32] studies a series of cure systems using an intrinsic fluorescence technique. Recently, Vatanparast and Hakala et al.[34] reported on the use of several fluorescence probes to follow the entire curing process. However, the fluorescence information was not directly correlated to the C═C bond

Scheme 3. Predominant Reaction Pathways for the Cure Reaction of Bismaleimide BMMA with 1,6-Diaminohexane: Michael Addition Reaction and Maleimide Homopolymerization

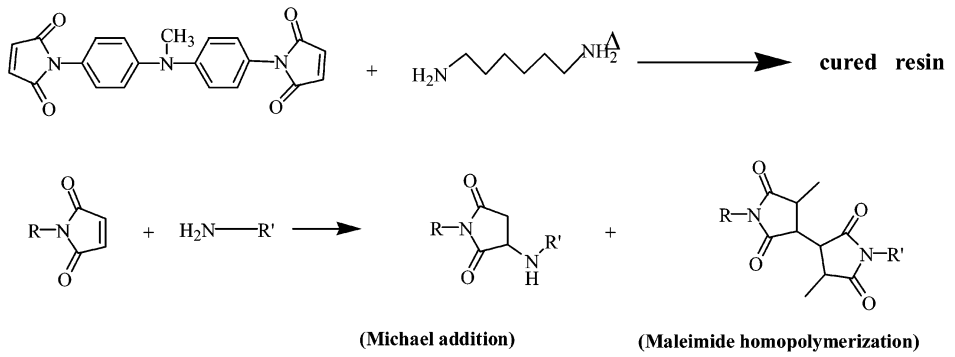

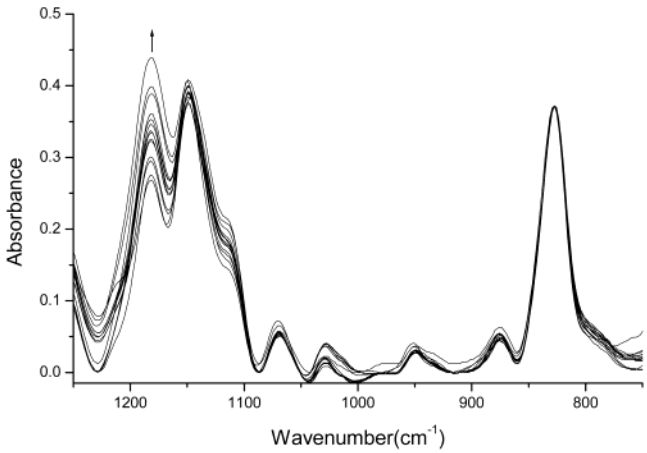

Figure 9. Variation of the C−N−C band intensity (1182 cm^{-1}) corresponding to the succinimide ring during the cure reaction.

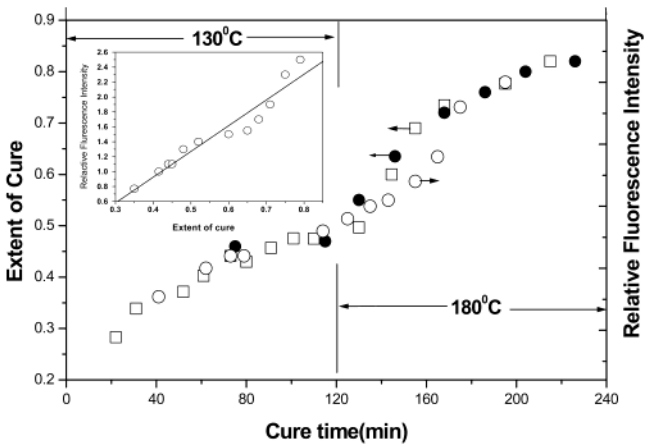

Figure 10. Cure reaction of BMMA with 1,6-diaminohexane monitored by means of FT-IR spectroscopy according to the change in the absorption band at 1182 (□) or 3101 cm^{-1} (●) and by following the changes in fluorescence intensity at 375.0 nm (○). Cure time schedules: at 130 (2 h) and 180 °C (2 h). Inset: Correlation plot between fluorescence intensity and the extent of cure.

conversion, and the fluorescence behavior was complex during cross-linking or curing.

In the following study, we attempt a further extension of the new fluorescence approach to the cure monitoring. The cure reaction of bismaleimide/diamine resins can yield a cross-linked network.[7] Here, an aliphatic 1,6-diaminohexane is chosen as a commoner in the cure reaction to avoid the interfering fluorescence of aromatic diamines. The cure reaction of an equimolar feed of BMMA and 1,6-diaminohexane was carried out at two stages: first, at 130 °C for 2 h; second, at 180 °C for 2 h.

In bismaleimide/diamine system, several reactions are possible.[7,30] The Michael addition or amine-maleimide chain extension reaction and the maleimide-maleimide cross-linking reaction are widely believed to be the predominant reactions occurring in the thermal cure reaction as shown in Scheme 3. Obviously, in both transformations proposed, the C═C bond of maleimide unit becomes saturated to form the succinimide unit.

A commonly used FT-IR method was employed to determine the extent of cure reaction of BMMA with 1,6-diaminohexane. Several distinct changes occur in the FT-IR spectra during the cure reaction. An absorbance band at 1182 cm^{-1} (corresponding to C−N−C succinimide resonance) increases due to the formation of succinimide ring as shown in Figure 9.

In addition, a decrease in 3101 cm^{-1} band was caused by the disappearance of the C−H vibrations of maleimide unit. The extent of the cure reaction based on the change in 1182 cm^{-1} or 3101 cm^{-1} band was calculated using eq 1 or eq 2.

$$\alpha = 1 - (A_{1182}/A_{827})_t/(A_{1182}/A_{827})_0 \quad (1)$$

or

$$\alpha = 1 - (A_{3101}/A_{827})_t/(A_{3101}/A_{827})_0 \quad (2)$$

The absorbance due to the phenyl group at 827 cm^{-1} (A_{827}) was used as an internal reference. The terms $(A_{1182}/A_{827})_t$ and $(A_{3101}/A_{827})_t$ are the absorbances at 1182 and 3101 cm^{-1} at cure time t corrected for thickness, respectively. The terms $(A_{1182}/A_{827})_0$ and $(A_{3101}/A_{827})_0$ are the absorbance at 1182 and 3101 cm^{-1} at cure time zero corrected for thickness, respectively.

The process of cure reaction was also monitored by following the change in fluorescence intensity. Figure 10 compares the fluorescence data with the IR data.

The correlation plot between the fluorescence intensity and the extent of cure is shown in the insetof Figure 10. The plot illustrated a linear relationship with a slight deviation occurring at 180 °C cure stage. This indicates that the fluorescence results are in agreement with the FT-IR results, however, there is a slight deviation at a high conversion stage. The slight deviation may be due to the multitude and complexity of the existing maleimide and succinimide formulation at finally cured state. The correlation plot can be used to estimate the extent of reaction. Therefore, the new fluorescence approach is also suitable for cure monitoring, which can directly reflect C═C bond consumption.

Conclusion

Bismaleimides and bisitaconimides having electron-donating diphenylmethylamine, triphenylamine, or 2,5-diphenyl-1,3,4-oxadiazole chromophore ($A_{(=)}-D_{(*)}-A_{(=)}$) as well as their saturated model compounds were synthesized. These $A_{(=)}-D_{(*)}-A_{(=)}$ monomers generally display a strong intramolecular fluorescence quenching. Their fluorescence quantum yields and lifetimes are always lower than those of their corresponding saturated compounds. The electron-poor C═C bond of maleimide and itaconimide units ($A_{(=)}$) plays a key role in the intramolecular quenching, which is correlated to the electron-accepting strength of $A_{(=)}$ and the geometry arrangement between $A_{(=)}$ and $D_{(*)}$. Furthermore, the absorption and emission of the charge-transfer complex were observed for BIPA, which revealed that the intramolecular quenching was attributed to an intramolecular charge-transfer interaction. The intramolecular charge-transfer mechanism is further confirmed by time-resolved fluorescence spectroscopy. An intermolecular fluorescence quenching study shows that the intramolecular quenching is a distinct mechanism from intermolecular interaction. On the basis of the strong intramolecular quenching of $A_{(=)}-D_{(*)}-A_{(=)}$ bismaleimides, a new fluorescence approach can be developed to monitor the process of polymerization and curing of bismaleimides, which can be employed not only by an intrinsic fluorescence technique but also by an extrinsic fluorescence technique. The advantage of the new fluorescence approach is that it provides information on the chemical structure of C═C bond, which is unavailable from the currently applied environment-sensitive fluorescence probe technique.

Acknowledgment. Financial support from the National Natural Science Foundation of China (No.5000-3001) and the Research Fund for the Doctoral Program of Higher Education (No 99000131) is gratefully acknowledged.

Supporting Information Available: Text and a scheme giving the synthetic procedures and spectral confirmations for BSMA, BSPA BIPA, *p*-BMPO, *p*-BSPO, *p*-BIPO, *m*-BMPO, *m*-BSPO, and *m*-BIPO, a figure showing Stern−Volmer plots for the fluorescence quenching of BSPA, BSMA, and *p*-BIPO by maleic anhydride and itaconic anhydride, and a figure showing ^{1}H NMR spectra during the model reaction of BMMA with isobutylamine. This material is available free of charge via the Internet at http://pubs.acs.org.

References and Notes

(1) For selected papers: (a) Hattemer, E.; Zentel, R.; Mecher, E.; Meerholz, K. *Macromolecules* **2000**, *33*, 1972−1977. (b) Marder, S. R.; Kippelen, B.; Jen, A. K. Y.; Peyghambarian, N. *Nature (London)* **1997**, *388*, 845−851. (c) Kim, S.; Park, S. Y. *Macromolecules* **2001**, *34*, 3947−3953. (d) Van, S. D.; Hendrickx, E.; Persoons, A. *Chem. Mater.* **2001**, *13*, 1230−1237. (e) Moon, H.; Hwang, J.; Kim, N.; Park, S. Y. *Macromolecules*, **2000**, *33*, 5116−5123.

(2) (a) Wu, S. K.; Li, F. M. In *New Trends In the Photochemistry of Polymers*; Allen, N. S., Rabek, J. F., Eds.; Elsevier, New York, 1985; p 85. (b) Wu, S. K.; Jin, Y. C.; Li, F. M. *Polym. Bull.* **1982**, *8*, 276−279. (c) Qiu, J.; Li, Z. C.; Gao, Q. Y.; Yao, G. Q.; Yang, G. X.; Zhang, J. X.; Li, F. M. *J. Polym. Sci., Polym. Chem.* **1996**, *34*, 3015−3023. (d) Li, F. M.; Gao, Q.Y.; Wang, L.; Zhang, J. X.; Chen, S. J.; Li, Z. C. *J. Polym. Sci., Part A: Polym. Chem.* **1997**, *35*, 1087−1093. (e) Zhang, X.; Du, F. S.; Li, Z. C.; Li, F. M. *Macromol. Rapid Commun.* **2001**, *22*, 983−987.

(3) (a) Du, F. S.; Cai, H.; Li, Z. C.; Li, F. M. *J. Polym. Sci., Polym. Chem*, **1998**, *36*, 1111−1116. (b) Du, F. S.; Li, Z. C.; Hong, W.; Gao, Q. Y. Li., F. M. *J. Polym. Sci., Polym. Chem.* **2000**, *38*, 679−688. (c) Du, F. S.; Li, Z. C. Li, F. M. *J. Polym. Sci., Polym. Chem.* **1999**, *37*, 179−187.

(4) Cumpston, B. H.; Ananthavel, S. P.; Barlow, S.; Dyer, D. L.; Ehrlich, J. E.; Erskine, L. L.; Heikal, A. A.; Kuebler, S. M.; Lee, I. Y. S.; McCord-Maughon, D.; Qin, J. Q.; Rockel, H.; Rumi, M.; Wu, X. L.; Marder, S. R.; Perry, J. W. *Nature* **1999**, *398*, 51−54.

(5) (a) Warman, J. M.; Abellon, R. D.; Verhey, H. J.; Verboeven, J. W.; Hofstraat, J. W. *J. Phys. Chem. B.* **1997**, *101*, 4913−4916. (b) Verhey, H. J.; Bekker, C. H. W.; Verhoeven, J. W.; Hofstraat, J. W. *New. J. Chem.* **1996**, *20*, 809−814.

(6) Cai, H.; He, X. H.; Zheng, D. Y.; Qiu, J.; Li, Z. C.; Li, F. M.*J. Polym. Sci., Part A: Polym. Chem.* **1996**, *34*,1245−1250.

(7) (a) Stenzenberger, H. D. Addition Polyimides. *Adv. Polym. Sci.* **1994**, *117*, 165−220. (b) Mison, P.; Sillion, B. Thermosetting Oligomers Containing Maleimides and Nadimides End-groups. *Adv. Polym. Sci.* **1999**, *140*, 137−179. (c) Patel, M. R.; Patel, S. H.; Patel, J. D. *Eur. Polym. J.* **1983**, *19*, 101−105. (d) White, J. E.; Scaia, M. D.; Snider, D. A. *J. Appl. Polym. Sci.* **1984**, *29*, 891. (e) Gherasim, M. G.; Zugravescu, I. *Eur. Polym. J.* **1978**, *14*, 985−990.

(8) (a) Loutfy, R. O. *Macromolecules* **1981**, *14*, 270−275. (b) Loutfy, R. O. *J. Polym. Sci., Part. B: Polym. Phys.* **1982**, *20*, 825−835. (c) Loutfy, R. O. *Macromolecules* **1983**, *16*, 678−680. (d) Jager, W. F.; Lungu, A.; Chen, D. Y.; Neckers, D. C. *Macromolecules* **1997**, *30*, 780−791. (e) Strehmel, B.; Strehmel, V.; Younes, M. *J. Polym. Sci., Part. B: Polym. Phys.* **1999**, *37*, 1367−1386.

(9) (a) *Applied Fluorescence in Chemistry, Biology and Medicine*; Rettig, W., Strehmel, B., Schrader, S., Seifert, H., Eds. Springer-Verlag: Berlin, 1999. (b) Winnik, F. M.; Regismond, S. T. A. *Colloid Surf. A* **1996**, *118*, 1−39. (c) *Photophysical and Photochemical tools in polymer science: Conformation, Dynamics, Morphology*; Winnik, M. A., Ed.; D. Reidel, Dordrecht; Holland, **1985.** (d) Rettig, W. *Top. Curr. Chem. Electron Transfer I* **1994**, 253−299. (e) Rettig, W.; Lapouyade, R. In *Topic in fluorescence Spectroscopy*; Lakowicz, J. R., Ed.; Plenum Press: New York, 1994; Volume 4: Probe Design and Chemical Sensing, pp 109−149. (f) Herbich, J.; Brutschy, B.; In *Electron Transfer in Chemistry;* Balzani, V., Ed.; Wiley-VCH: New York; 2001; pp 697−741.

(10) (a) Phelan, J. C.; Sung, C. S. P. *Macromolecules* **1997**, *30*, 6845−6851. (b) Phelan, J. C.; Sung, C. S. P. *Macromolecules* **1997**, *30*, 6837−6844.

(11) Saegusa, Y.; Koshikawa, T.; Nakamura, S. *J. Polym. Sci., Part A Polym. Chem.* **1992**, *30*, 1369−1373.

(12) (a) Gorvin, J. H. *J. Chem. Soc., Perkin Trans. I.* **1988**, 1331−1335. (b) Kloetzel, M. C.; Davis, S. J.; Pandit, U. *J. Med. Pharm. Chem.* **1959**, *1*, 197−211. (c) Pachter, I. J.; Kloetzel, M. C. *J. Am. Chem. Soc.* **1952**, *74*, 1321−1322. (d) Oishi, Y.; Ishida, M.; Kakimoto, M. A.; Imai, Y.; Kurosaki, T. *J. Polym. Sci., Part A: Polym. Chem.* **1992**, *30*, 1027−1035. (e) Oishi, Y.; Takado, H.; Yoneyama, M.; Kakimoto, M. A.; Imai, Y. *J. Polym. Sci., Part A: Polym. Chem.* **1990**, *28*, 1763−1769. (f) Wang, C.; Zhang, C.; Wang, P.; Zhu, P.; Wu, W.; Ye, C.; Dalton, L. R. *Polymer* **2000**, *41*, 2583−2590. (g) Kudo, M.; Fujimoto, M. J P Patent 02,306,960. 1990 (*Chem. Abstr.* **1991**, *114*, 247955q).

(13) Fluorescence quantum yields were calculated from the integrated intensity under the emission band (A) using the following equation: $\phi = \phi_r (A/A_r)(\mathrm{OD}_r/\mathrm{OD})(n^2/n_r^2)$, where OD is the optical density of the solution at the excitation wavelength, and n is the refractive index. The optical density of the solution for the calculation of quantum yields was less than 0.1 at the excitation wavelength. The solvent 9,10-diphenylanthrene in cyclohexane was used as reference ($\phi_r = 0.90$) (Eaton, D. F. *Pure. Appl. Chem.* **1988**, *60*, 1107−1114).

(14) Electron affinity (EA) of acrylamide was calculated from the known $E_{1/2}^R$ (−1.97 V) (Macwilliaws, D. C.; Kaufman, D. C.; Waling, B. F. *Anal. Chem.* **1965**, *37*, 1546−1551) using the relationship of Chen (Chen, E. C. M.; Wentworth, W. E. *J. Chem. Phys.* **1975**, *63*, 3183−3191).

(15) (a) Kwok, C. C.; Wong, M. S. *Macromolecules.* **2001**, *34*, 6821−6830. (b) Schulz, B.; Bruma, M.; Brehmer, L. *Adv. Mater.* **1997**, *9*, 601−613. (c) Hemming, K. *J. Chem. Res-S*, **2001**, 209−216.

(16) Paul, G.; Kebarle, P. *J. Am. Chem. Soc.* **1989**, *111*, *464*−470.

(17) (a) Lami, H.; Laustriat, G. *J. Chem. Phys.* **1968**, *48*, 1832−1840. (b) Michael, P. R.; Faulkner, L. R. *J. Am. Chem. Soc.* **1977**, *99*, 7754−7761.

(18) (a) Lakowicz, J. R. *Principles of Fluorescence Spectroscopy*, 2nd ed.; Plenum Press: New York, 1999; p 239. (b) To avoid the inner filter effects due to the absorption of the incident light and the emitted light, the fluorescence intensity was corrected as follow: $I = I_{obs} \times 10^{[(ODex+ODem)/2]}$ I_{obs} is the observed fluorescence intensity. OD_{ex} and OD_{em} are the optical densities at excitation and emission wavelength, respectively.
(19) Hoefnagel, A. J.; Hoefnagel, M. A. Wepster, B. M. *J. Org. Chem.* **1981**, *46*, 4209−4211.
(20) Stroeks, A.; Shmorhun, M.; Jamieson, A. M.; Simha, R. *Polymer* **1988**, *29*, 467−470.
(21) Miller, K. E.; Burch, E. L.; Lewis, F. D, Torkelson, J. M. *J. Polym. Sci., Part. B: Polym. Phys.* **1994**, *32*, 2625−2635.
(22) (a) Jager, W. F.; Sarker, A. M.; Neckers, D. C. *Macromolecules* **1999**, *32*, 8791−8799. (b) Jager, W. F.; Norder, B. *Macromolecules* **2000**, *33*, 8576−8582.
(23) Pankasem, S.; Biscoglio, M.; Thomas, J. K. *Langmuir* **2000**, *16*, 3620−3625.
(24) (a) Li, F. M.; Chen, S. J.; Li, Z. C.; Qiu, J. *J. Polym. Sci., Polym. Chem.* **1996**, *34*, 1881−1888. (b) Peinado, C.; Alonso, A.; Salvador, E. F.; Baselga, J.; Catalina, F. *Polymer* **2002**, *43*, 5355−5361.
(25) Crivello, J. V. *J. Polym. Sci., Polym. Chem.* **1973**, *11*, 1885−1200.
(26) Winnik, F. M. *Chem. Rev.* **1993**, *93*, 587−614.
(27) (a) Agag, T.; Takeichi, T. *Macromolecules* **2001**, *34*, 7257−7263. (b) Grubbs, R. B.; Dean, J. M.; Broz, M. E.; Bates, F. S. *Macromolecules* **2000**, *33*, 9522−9534. (c) Wright, M. E.; Schorzman, D. A.; Pence, L. E. *Macromolecules* **2000**, *33*, 8611−8617. (d) Hattemer, E.; Zentel, R.; Mecher, E.; Meerholz, K. *Macromolecules* **2000**, *33*, 1972−1977.
(28) (a) Wright, M. E.; Schorzman, D. A.; Pence, L. E. *Macromolecules* **2000**, *33*, 8611−8617. (b) Hopewell, J. L.; George, G. A.; Hill, D. J. T. *Polymer* **2000**, *41*, 8221−8229. (c) Dollimore, D.; Phang, P. *Anal. Chem.* **2000**, *72*, 27−36.
(29) (a) Kim, K. H.; Jang, S.; Harris, F. W. *Macromolecules* **2001**, *34*, 8925−8933. (b) Yu, J. W.; Sung, C. S. P. *Macromolecules* **1995**, *28*, 2506−2511. (c) Kailani, M. H.; Sung, C. S. P.; Huang, S. J. *Macromolecules* **1992**, *25*, 3751−3757.
(30) (a) Curliss, D. B.; Cowans, B. A.; Caruthers, J. M. *Macromolecules* **1998**, *31*, 6776−6782. (b) Okumoto, S.; Yamabe, S. *J. Org. Chem.* **2000**, *65*, 1544−1548.
(31) (a) Hopewell, J. L.; Hill, D. J. T.; Pomery, P. J. *Polymer* **1998**, *39*, 5601−5607. (b) Brown, I. M.; Sandreczki, T. C. *Macromolecules* **1990**, *23*, 94−100.
(32) (a) Wang, S. K.; Sung, C. S. P. *Macromolecules* **2002**, *35*, 877−882. (b) Wang, S. K.; Sung, C. S. P. *Macromolecules* **2002**, *35*, 883−887. (c) Yu, J. W.; Sung, C. S. P. *Macromolecules* **1997**, *30*, 1845−1846. (d) Sun, X. D.; Sung, C. S. P. *Macromolecules* **1996**, *29*, 3198−3202. (e) Xu, Y. E.; Sung, C. S. P. *Macromolecules* **2002**, *35*, 9044−9048.
(33) Strehmel, B.; Malpert, J. H.; Sarker, A. M.; Neckers, D. C. *Macromolecules* **1999**, *32*, 7476−7482.
(34) (a) Hakala, K.; Vatanparast, R.; Li, S. Y.; Peinado, C.; Bosch, P.; Catalina, F.; Lemmetyinen, H. *Macromolecules* **2000**, *33*, 5954−5959. (b) Vatanparast, R.; Li, S. Y.; Hakala, K.; Lemmetyinen, H. *Macromolecules* **2000**, *33*, 438−443.

MA0205111